Fuzzy Based Active and Reactive Power Support to the Distribution Network Using Electric Vehicles

Kannan Thirugnanam, *Member, IEEE*
Dept. of EPD, SUTD, Singapore,
Singapore-487372. E-mail:kannan.thirugnanam.phd@ieee.org

Praveen Kumar, *Member, IEEE*
Dept. of EEE, Indian Institute of Technology Guwahati,
Assam - 781039. E-mail: praveen kumar@iitg.ernet.in

***Abstract*— Due to increasing peak power demand and decreasing quality of power delivery to consumers, the penetration of Electric Vehicles (EVs) are highly acceptable for grid support. If the EVs are exchange active and reactive power to grid during parking hours, then the peak power demand has reduced and quality of power delivery has improved. The EVs are discharged at a place to be called as a Grid Supporting Station (GSS). The GSS have multiple Discharging Units (DUs) which transfers active and reactive power from EVs' batteries to grid. In this paper, a fuzzy based control method is described for EVs which regulate the active and reactive power for grid support. The active and reactive power flow from EVs to grid based on the node voltage and amount of energy available in the GSS. Each DU is designed for a maximum power handling capacity of 80VA. The performance of the GSS is analyzed with five set of EVs which is connected through point of Common Coupling (PCC) of distribution node. Simulation studies show that the GSS could effectively exchange the power for grid support during the peak hours.**

***Index Terms*— Active and reactive power, battery, electric vehicles, grid connected inverter, fuzzy logic controller, vehicle to-grid.**

I. Introduction

Depleting natural oil and fossil fuel, the Electric Vehicles (EVs) have received considerable attention in the recent years [1], [2]. The EVs are growing in popularity due to eco-friendly and cost effective over conventional vehicle driven by internal combustion engine [3]. With the wide spread integration of EVs into electric grid, the Vehicle-to-Grid (V2G) system has becomes one of the key issue which enables the EVs have ability to provide energy back to grid during parking hours. During these hours, large number of EVs can be represented as a distributed energy source which can able to eliminate the peak power demand. Therefore, it is required to develop a system which can able to handle the large penetration of EVs to support the grid during peak hours also improve the power quality. During peak hours, the Distribution Node (DN) voltage gets reduced due to fluctuations of the reactive load which gives adverse impacts to the DN [4], [5]. Therefore, voltage is one of the most important elements for power quality [4]. To address these issues, the EVs can able to provide active as well as reactive power support, then the DN voltage drop and power quality to consumers has been improved during peak power demand. This is realized, the aggregated EVs' energy is used in controlled manner to discharge the stored energy to the grid [6]. This can be archived when the Grid Supporting Station (GSS) is situated near the DN in the parking bay. The parking bay can be a plug-in point or office complex or Industrial area. In the parking bay, the EVs are expected to be available for longer duration about 5-6 hours a day [1]. During these hours, EVs provide energy fed back to DN based on the DN voltage (V_n), energy availability of GSS (E_{gss}), constraints of the EV battery such as state of charge and discharge rates. Therefore, the GSS can be designed to handle large number of EVs and it is operated in controlled and coordinated manner, the peak power demand has been reduced.

In literature, many works has been reported where the renewable energy sources are used to provide active and reactive power to grid [7]–[9]. A combined problem formulation for active and reactive optimal power flow in DNs with embedded wind generation and energy storage system has been discussed [10]. Many researchers have developed shunt active filter to regulate the power delivery to consumers [11]–[13]. In most of the work, a centralized Control Strategies (CS) has been developed which can control the active and reactive power to grid [14], [15]. A direct power CS for grid connected converters have been discussed [14]–[16]. An optimal charging station and CS has been developed which can support the power to electric grid using Fuzzy Logic Controller (FLC) for regulating the voltage and peak shaving [17], [18]. The concept of multi charging station based on active power control has been discussed in [19] to support the grid by charging or discharging the EVs' batteries throughout a day. These control approaches aims at the effective utilization of EVs for grid support. With the larger penetration of EVs, the energy stored in EVs' batteries are capable of providing active power as well as reactive power for stabilizing the DN voltage and improve the power quality, which has been studied in this work. Therefore, this work is mainly focused on the following issues:

- Design and simulation of GSS with its associated controller to coordinate large fleet of EVs' batteries.
- Analysis the behaviour of GSS with active and reactive power support by controlling the power angle and voltage. • MATLAB Simulink model have been developed based on the real time data of Guwahati city, Assam, India.

The GSS considered in this work has many Discharging Units (DU), where multiple EVs arrive to discharge their batteries. In such case, the GSS should have sufficient control mechanism to coordinate multiple EVs, to handle the sudden arrival and departure of EVs. A Fuzzy Logic Controller (FLC) and an aggregator is used in the GSS for achieving the control and coordination of the complete system which is shown in Fig. 1. The GSS controller decides the net power (S_{ent}) to be support to the DN. The aggregator distributes the power ($S^1_{ref}, S^2_{ref} \ldots S^n_{ref}$) among EVs of different ratings. Here, n is the number of EVs present in the GSS. The main idea of this work is to drawn necessary power from EVs to mitigate the peak power demand and improve the power delivery. To

demonstrate the importance of proposed approach, a real-time distribution system data of Guwahati city is used. Simulation has been done to prove the validity of the approach, which has been tested with 5 EVs of different ratings.

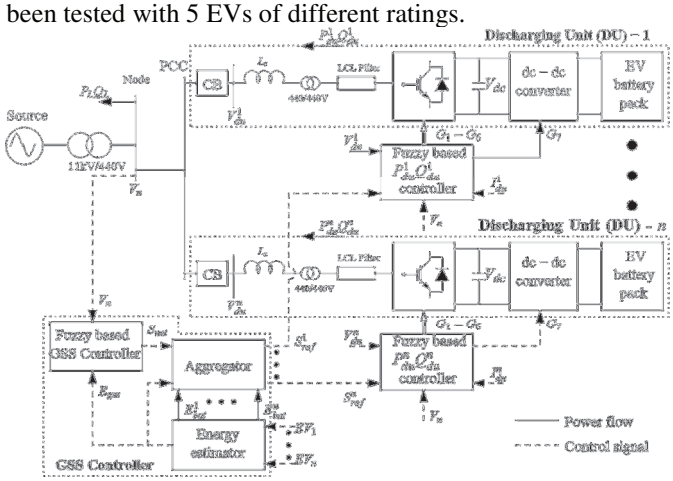

Fig. 1: Schematic representation of grid connected EVs.

The paper is organized as follows: Section II presents the background of active (P^n_{du}) and reactive (Q^n_{du}) power control. Modelling of the grid supporting station, EV battery, circuit diagram of the individual DU and fuzzy based $P^n_{du}Q^n_{du}$ - controller has been explained in Section III. The FLCs are discussed in Section IV. Simulation results are discussed in Section V and the conclusion is given in Section VI.

II. Background

In practice, the voltage drop in the DN can be regulated by injecting active and reactive power from the EVs. The concept of power exchange between the GSS and DN is explained through the simple circuit which is given Fig. 2. Assuming, the power flow happens from the GSS to the DN, the voltage injected from the n^{th} DU is $V^n_{du}$and voltage at the DN is V_n.

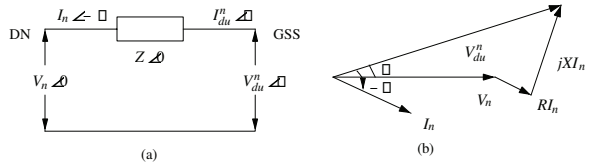

Fig. 2: Single line diagram of DN and GSS (a) power flow through a line (b) phasor diagram [9], [20].

The power flow from GSS to DN is given in Fig. 2. The mathematical representation is given in Eq. (1) [20].

$$P + jQ = \frac{V_n^2}{Z} e^{j\theta} - \frac{V_n V^n_{du}}{Z} e^{j(\theta+\delta)} \quad (1)$$

The active and reactive power flow through a line is given in Eq. (2) and Eq. (3) which is simplified from Eq. (1) [20].

$$P^n_{du} = \frac{V_n^2}{Z}\cos\theta - \frac{V_n V^n_{du}}{Z}\cos(\theta+\delta) \quad (2)$$

$$Q^n_{du} = \frac{V_n^2}{Z}\sin\theta - \frac{V_n V^n_{du}}{Z}\sin(\theta+\delta) \quad (3)$$

The n^{th} discharging unit active ($P_{du}{}^n$) and reactive (Q^n_{du}) power is derived from Eq. (2) and Eq. (3). The simplified equation for $P^n_{du}$and $Q^n_{du}$is given below.

$$P^n_{du} = \frac{V_n V^n_{du}}{X}\sin(\delta) \quad (4)$$

$$Q^n_{du} = \frac{V^n_{du}}{X}(V^n_{du} - V_n\cos(\delta)) \quad (5)$$

The amount of active power injected at the DN is controlled by varying power angle (□). The power flow from GSS to the DN occurs when the GSS voltage leads the DN voltage. The maximum active power transfer happens, when □ = 90□. From Eq. (4) and Eq. (5), the power angle depends on P^n_{du}, the n^{th} DU and DN voltage difference (V^n_{du}- V_n) depends on Q^n_{du}[9], [20]. Therefore, the P^n_{du}can be controlled by regulating □ and Q^n_{du}can be controllable by adjusting n^{th} DU voltage.

III. Modeling of the System

A. Distribution network

The redial distribution system of Guwahati city, Assam, India is shown in Fig. 3. It comprises of 33kV, 5MVA main feeder and four 11kV/440V distributed sub feeder, typically operated in a radial fashion. The reduced data of this network has been taken for this study and the load in the system is varying with respect to time. The GSS considered for this study has been connected to the DN (33) of Aminga on Industrial Area (AIA). The GSS exchange the active and reactive power to DN during peak hours of the AIA.

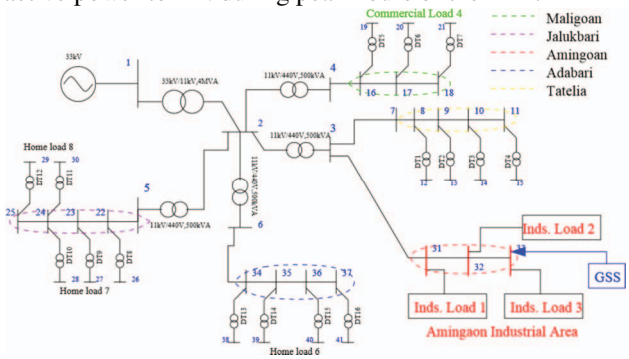

Fig. 3: Distribution network of Guwahati City.

B. EVs Battery Modelling

The EVs battery can be represented in terms of electric equivalent circuit (EEC) [18]. The simple EEC has been used in this work which have internal resistance (R_1), capacitance (C) and open-circuit voltage (V_0) [21]. The EEC based Simulink model of EV battery is given in Fig. 4.

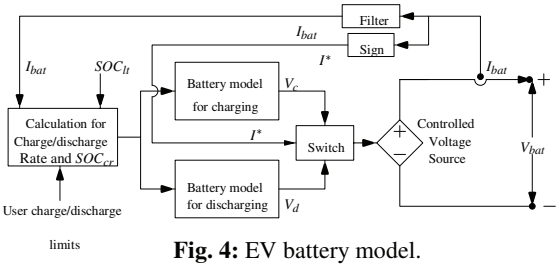

Fig. 4: EV battery model.

This model is charge or discharge based on the reference current (I^*). The battery terminal voltage for charging and discharging scenario has been given in [21]. The EVs battery model neither charge nor discharge based on user specified limits. For the constant discharge current, the current State of-Charge (SOC_{cr}) of the battery is calculated from Eq. (6).

$$SOC^n_{cr} = SOC^n_{lt} + \frac{I^n_{bat}\Delta t^n}{3600Q^n} \quad (6)$$

where, n is the number of EVs present in the GSS, I^n_{bat} is the n^{th} EVs discharge current (A), Δt^n is the n^{th} EVs change in time for discharge operation (*Sec*) and Q^n is the n^{th} EVs nominal capacity (*Ah*). The available energy of the n^{th} EVs' batteries (E^n_{bat}) is given in Eq. (7).

$$E^n_{bat} = V^n_{bat} Q^n \Delta SOC^n_{cr} \quad (7)$$

where, ΔSOC^n_{cr} is the change in SOC_{cr}. The total energy of the GSS (E_{gss}) can be estimated from Eq. (8).

$$E_{gss} = \sum_{i=1}^{m} E^n_{bat_i} \qquad m = 1, 2 \ldots n \quad (8)$$

C. Grid Supporting Station

The GSS is a place where EVs can discharge their battery energy in controlled and coordinated manner. A schematic block diagram of grid connected Discharging Unit (DU) is given in Fig. 1. It consists of GSS controller, aggregator, $P^n_{du}Q^n_{du}$ controller and DU which transfer the power from EVs' batteries to DN. The exchange of power from EVs' batteries to DN, the n^{th} DU should be synchronizing with DN. The voltage of the n^{th} DU and frequency should match with the DN for proper synchronization. To satisfy this condition, the EVs' batteries arrive at the GSS would discharge some energy initially for synchronizing with the DN. During synchronization period, there is no power transfer from EVs' batteries to DN. There will be a small negative flow of current during synchronization period. This is because, the EVs arrive at the GSS will make a closed path through converters switches having low resistance and there is some initial current flow through L_1CL_2 filter and this consumes very less power. The GSS controller decide the total power (S_{net}) required to discharge the EV battery for grid support. The GSS controller decide magnitude based on E_{gss} and the V_n. The GSS aggregator distribute the reference power (S^n_{ref}) to n^{th} DU based on the S_{net}, E_{gss} and E^n_{bat} [17], [18].

D. Circuit Topology of the n^{th} Discharging Unit

The circuit topology of the n^{th} DU is given in Fig. 5. The n^{th} DU consist of EV battery pack, dc to dc converter, dc to three phase ac converter, L_1CL_2 filter, Transformer (Tf) and Circuit Breaker (*CB*). To regulate the power flow, fuzzy based control strategies have been developed. Based on the aggregator control signal, the $P^n_{du}Q^n_{du}$ FLC decide the □ and duty cycle for the corresponding converter. The detail description of the $P^n_{du}Q^n_{du}$ FLC is given in next section.

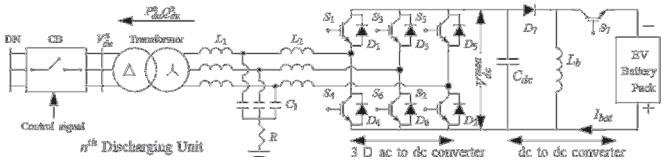

Fig. 5: Circuit topology of the n^{th} discharging unit.

The Simulink model of the GSS has been developed and validated with the test system of Guwahati city, Assam, India. The parameter specifications are given in Table I.

TABLE I: Parameters specifications of n^{th} discharging unit.

Parameter	Descriptions	Values
L_1CL_2	3 □ filter circuit	0.6mH, 0.08mF, 0.8mH
C_b	dc link capacitor	20mF
L_b	dc-dc converter inductance	0.28mH
X,R	Filter resistance, reactance	2Ω 2.42Ω

The following assumptions have been made for power flows from EVs' batteries to DN:

- Each discharging unit of the GSS is designed for maximum power handling capacity of 80kW.
- The GSS is placed near to the distribution node Amingaon Industrial Area (**Node 33**).
- Five EVs' batteries are considered in this work, with the capacity of 32kWh, 34kWh, 40kWh, 48kWh and 54kWh. Capacity losses of the EVs' batteries are not considered.

E. Fuzzy Based $P^n_{du}Q^n_{du}$ Controller

A diagram of the implemented P^n_{du} Q^n_{du} power control strategy is given in Fig. 6. The GSS aggregator is distribute the S^n_{ref} to n^{th} DU which is emphasized in Fig. 6. The power factor correction block is used to generate active (P^n_{ref}) and reactive (Q^n_{ref}) power reference signal. Based on *pq−theory* [22], the n^{th} DU Q^n_{du} and Q^n_{dy} power is estimated by using Clarke transformation [11].

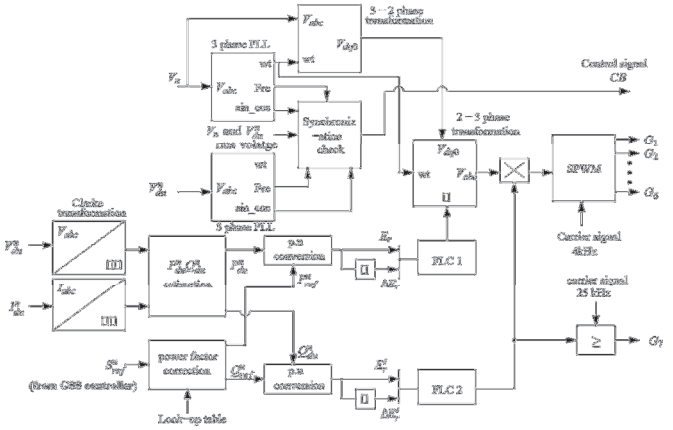

Fig. 6: Fuzzy based $P^n_{du}Q^n_{du}$ control strategy.

The reference and estimated signals are converted into per unit (p.u.) which is given into to FLC-1 and FLC-2. The FLC-1 and FLC-2 decide the power angle (□) and duty cycle for dc to three phase ac converter and dc to dc converter, respectively. The *abc−dqo* transformation is used to convert n^{th} DU voltage (V^n_{du}) to two phase (V_{dq0}) reference signal [12], [22]. The estimated □ is added with two phase signals by using inverse Park Transformation [12] which is reference signal for Sine Pulse Width modulation (SPWM). Synchronization block is used to turn-on the *CB*. The DN and n^{th} DU voltage and frequency are equal, then the *CB* is turn-on else it is remain open circuit.

IV. Fuzzy Logic Controllers

Fuzzy logic derived from fuzzy set theory which can deal with uncertainties in systems. Fuzzy logic incorporates a simple, IF-THEN rule based approach to solve a control problem rather than attempting to mathematically model a

system [17], [23]. The crisp inputs are converted into grades of membership for linguistic terms of fuzzy sets by using the fuzzification [19]. The rule base collects the control rules which describe expert's knowledge and experience in the fuzzy set. Based on the rule base and fuzzification values, the fuzzy control values have been generated in the inference engine.

A. Defuzzification

Defuzzification is a method which convert fuzzy output into crisp output. The general expression for defuzzification is given in [23]. Mamdani type inference is used here for the implication of rules. In order to achieve a fast and accurate result, center of gravity method is chosen for defuzzification.

1) ***GSS Controller****:* : Seven fuzzy subsets such as Small (S), Very Low (VL), Low (L), Medium (M), High (H), Very High (VH) and Big (B) have been chosen for the inputs ($V_n$and E_{cs}) and output (S_{cs}) variables.

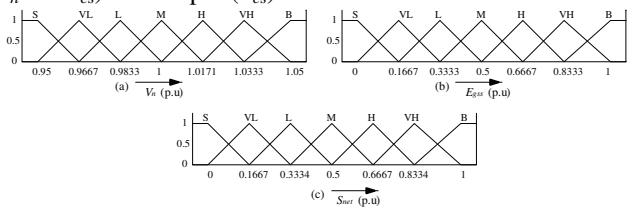

Fig. 7: Fuzzy membership function of GSS controller.

The membership function for GSS controller is given in Fig. 7 and rule base is given in Table II. When the $V_n$is VL (0.96667p.u) and the $E_{gss}$is VH (0.8333 p.u), then the FLC output will be VH (0.08334 p.u). Similarly, the remaining rules are developed for GSS controller.

2) P^n_{du} Q^n_{du}***Controller****:* : The linguistic represent of the FLC-1 is Negative High (NH), Negative Small (NS), Zero (Z), Positive Small (PS) and Positive High (PH) have been chosen for the Error (E_r) and Error Rate ($E\Delta_r$).

TABLE II: Rule base for GSS controller.

$V_n\rightarrow$ $E_{cs}\downarrow$	S	VL	L	M	H	VH	B
S	S	S	S	S	S	S	S
VL	VL	VL	VL	S	S	S	S
L	L	L	L	S	S	S	S
M	M	M	M	VL	S	S	S
H	H	H	H	VL	S	S	S
VH	VH	VH	VH	L	S	S	S
B	B	B	B	L	S	S	S

Five fuzzy subsets has been used for output such as Very Small (VS), Small (S), Medium (M), Big (B) and Very Big (VB). The membership function and rule base is given in Fig. 8 and Table III. The rule base has been developed based on the Eq. (4) and Eq. (5). When the $E_r$is NH (−1) and $E\Delta_r$is PS (0.2) which means the P^n_{du} is greater than the P^n_{ref}, then the power angle decided by the FLC is VS. Similar type of rule base and membership function has been used for duty cycle controller (FLC-2).

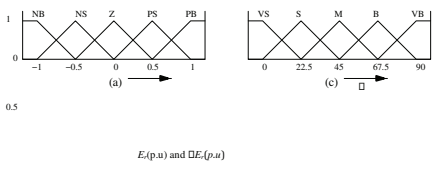

Fig. 8: Fuzzy membership function of power angle controller (a) inputs: $E_r$and ΔE_r(b) output: .

TABLE III: Rule base for power angle controller.

$E_r\rightarrow$ $\Delta E_r\downarrow$	NB	NS	Z	PS	PB
NB	VS	VS	S	S	M
NS	VS	S	S	M	B
Z	S	S	M	B	B
PS	S	M	B	B	VB
PB	M	B	B	VB	VB

V. RESULT AND DISCUSSION

To investigate the power control behaviour of the GSS, five EVs' batteries are taken for representing the bulk discharging of EVs. The total size of GSS studied in this work having maximum peak power handling capacity on 400VA. For simplification of analysis, EVs' batteries are same voltage ratings (250V), different energy rating and SOC_{cr}. The specifications of EVs' batteries are given in Table IV.

TABLE IV: Specifications of EVs' batteries

.

EVs	Energy (kWh)	Nominal Voltage(V)	SOC_{lt}	SOC_{cr}	C_r/D_r
EV_1	24	250	90	85	3.0
EV_2	28	250	80	90	2.5
EV_3	32	250	95	82	3.5
EV_4	40	250	85	88	2.5
EV_5	48	250	80	87	4.0

In active and reactive power control has been analyzed, to study the peak power mitigation and improve the power quality. The system operation is tested during peak hours, when the node voltage is generally low (below 0.9833 p.u). A total of 245.48*VA* is transferred from EVs' batteries to DN during the peak power demand hours. To show the dynamics of the system, the simulation results are shown for 0.5 seconds.

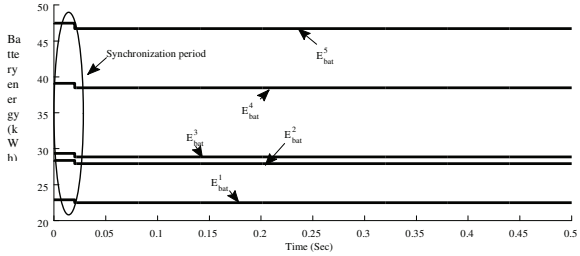

Fig. 9: EVs' batteries energy (kWh).

The energy availability of the EVs' batteries from E^1_{bat} to E^5_{bat} is given in Fig. 9. It is evident from the figure, the GSS controller decides a total of 249.57*VA* of power to support the DN by using EVs' which is parked in the parking bay.

Fig. 10 shows the simulated curves of EVs' batteries power (P^1_{bat} to P^5_{bat}). It is very clear from the figure, the sign of power is negative which means the EVs' batteries are supporting the DN during parking hours.

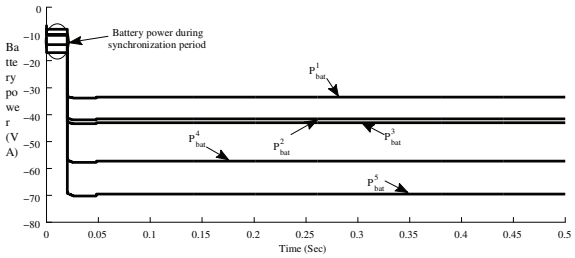

Fig. 10: EVs' batteries power (VA).

The EVs' batteries current *SOC* (SOC_{cr}) is shown in Fig. 11. The battery $SOC_{cr}$is decreasing due to injecting the energy from EVs' batteries.

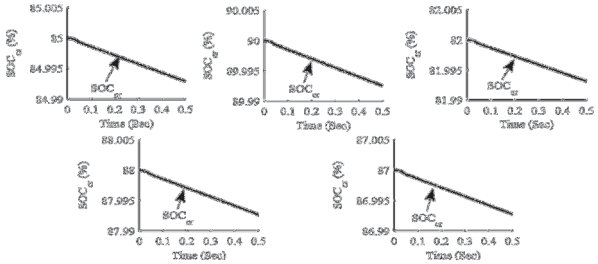

Fig. 11: Battery current State of charge (%).

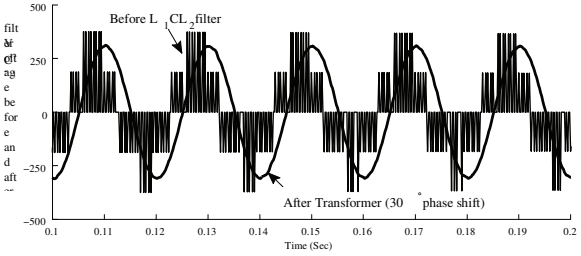

Fig. 12: Before and after the filter voltage (V).

The comparison of filtered and unfiltered voltage of the inverter during grid supporting hours is shown in Fig. 12. The square wave output waveform of inverter can inject harmonics in the grid voltage. The filtered output waveform has a total harmonic distortion of 2.59% which is inacceptable level of IEEE519 standard for harmonic limits.

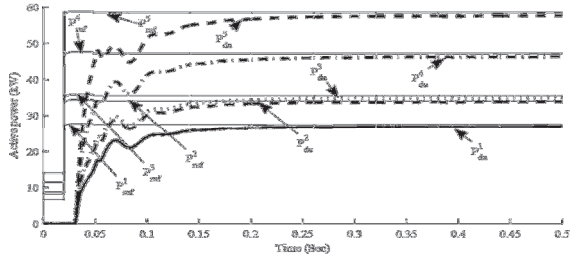

Fig. 13: Reference and estimated active power (kW).

Fig. 13 shows the comparison of reference (P^1_{ref} to P^5_{ref}) and estimated (P^1_{du} to P^5_{du}) active power of the individual DU. The summary of power transfer from EVs' batteries to DN during peak power demand hours is given in Table V.

The comparison of reference (Q^1_{ref} to Q^5_{ref}) and estimated (Q^1_{du} to Q^5_{du}) reactive power of the each DU is shown in Fig. 14. The total 143.94kVar of reactive power have been transferred from EVs' batteries to DN to improve the power quality. Due to bulk transfer of reactive power support to grid, the $V_n$have been improved which is shown in Fig. 16.

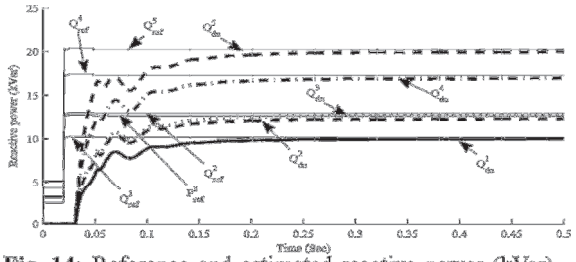

Fig. 14: Reference and estimated reactive power (kVar).

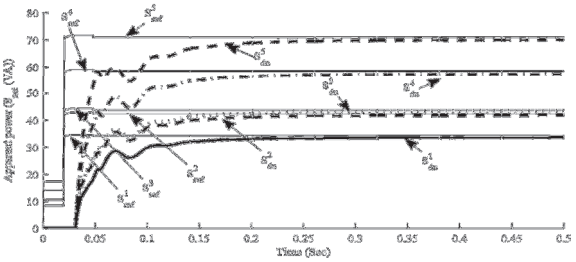

Fig. 15: Reference and estimated apparent power (VA).

Fig. 15 shows the comparison of reference (S^1_{ref} to S^5_{ref}) and estimated (S^1_{du} to S^5_{du}) apparent power of the each DU. The net power flow from EVs batteries to DN is 245.48*VA* but the GSS controller has decide 247.09*VA*. There is a small difference in the injected battery power and power at PCC, due to losses in the system. The power losses due to the internal resistance of converter, transformer and filter circuit.

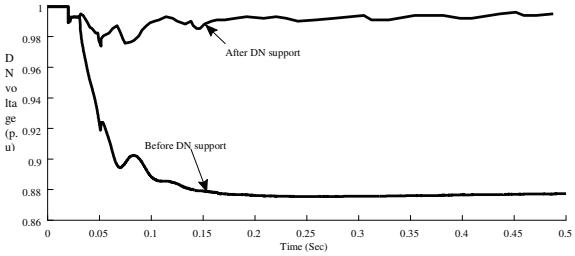

Fig. 16: DN voltage - before and after grid support (p.u).

Fig. 16 shows the node voltage (V_n) before and after DN support. Initially, the DN voltage has dropped much due to peak load. The voltage is increased from 0.8675p.u to 0.995p.u. From Fig. 9 to Fig. 16, due to DN support, the voltage profile also improved and the quality of the power delivery have been increased.

TABLE V: Summary of power transfer from EVs' batteries to DN during peak power demand (DU_1 to DU_5).

EV battery		Active power		Reactive power		Apparent power	
E_{bat} (kWh)	P_{bat} (VA)	P_{ref} (kW)	P_{du} (kW)	Q_{ref}(kVar)	Q_{du} (kVar)	S_{ref}(VA)	S_{net}(VA)
22.51	-34.14	27.51	26.99	20.33	19.95	34.21	33.49
27.93	-42.46	34.11	33.92	25.29	24.55	42.44	41.78
28.88	-43.79	35.54	34.96	25.74	25.74	43.88	43.08
38.47	-58.39	47.17	46.25	34.52	33.84	58.45	57.21
46.73	-71.09	58.38	57.57	40.44	39.89	71.01	69.92
164.52	-249.81	202.71	199.69	145.09	143.97	247.09	245.48

VI. CONCLUSION

In this work, a GSS has been modelled at component level with its controller and an aggregator to mitigate the peak power demand at the DN. The control algorithm has been designed for the GSS, which controls the active and reactive power flow from GSS to DN, by changing the power angle

and duty ratio of the converter. Simulation study has been performed considering a Real-time distribution system of Guwahati city. The analysis shows that the active and reactive power support has significant impact on flattening the voltage profile and reduced the peak power demand with EVs' batteries constraints. The proposed control is very efficient in performance since it provides better voltage control while managing the EVs battery in the GSS.

REFERENCES

[1] J. Tomic and W. Kempton, "Using fleets of electric-drive vehicles for grid support," *J. Power Sources*, vol. 168, no. 2, pp. 459–468, Jun. 2007.

[2] Y. Ma, T. Houghton, A. Cruden, and D. Infield, "Modeling the benefits of vehicle-to-grid technology to a power system," *IEEE Trans. Power Syst.*, vol. 27, no. 2, pp. 1012 –1020, May 2012.

[3] Z. Darabi and M. Ferdowsi, "Aggregated impact of plug-in hybrid electric vehicles on electricity demand profile," *IEEE Trans. Sustain. Energy*, vol. 2, no. 4, pp. 501–508, Oct. 2011.

[4] Z. Yang, S. Yu, W. Lou, and C. Liu, "Privacy-preserving communication and precise reward architecture for V2G networks in smart grid," *IEEE Trans. Smart Grid*, vol. 2, no. 4, pp. 697 –706, Dec. 2011.

[5] N. Rotering and M. Ilic, "Optimal charge control of plug-in hybrid electric vehicles in deregulated electricity markets," *IEEE Trans. Power Syst.*, vol. 26, no. 3, pp. 1021–1029, Aug. 2011.

[6] M. Ortega-Vazquez, F. Bouffard, and V. Silva, "Electric vehicle aggregator/system operator coordination for charging scheduling and services procurement," *IEEE Trans. Power Syst.*, vol. 28, May 2013.

[7] A. Moawwad, V. Khadkikar, and J. Kirtley, "A new P - Q - V droop control method for an interline photovoltaic (I-PV) power system," *IEEE Trans. Power Delivery*, vol. 28, no. 2, pp. 658–668, Apr. 2013.

[8] F. Wang, J. Duarte, and M. Hendrix, "Active and reactive power control schemes for distributed generation systems under voltage dips," *in Proc. IEEE Energy Conver. Cong. and Expo.*, pp. 3564–3571, Sept. 2009.

[9] L. Xu and P. Cartwright, "Direct active and reactive power control of DFIG for wind energy generation," *IEEE Trans. Energy Convers.*, vol. 21, no. 3, pp. 750–758, Sept. 2006.

[10] A. Gabash and P. Li, "Active-reactive optimal power flow in distribution networks with embedded generation and battery storage," *IEEE Trans. Power Syst.*, vol. 27, no. 4, pp. 2026–2035, Non. 2012.

[11] H. Akagi, H. Fujita, and K. Wada, "A shunt active filter based on voltage detection for harmonic termination of a radial power distribution line," *Industry Applications, IEEE Transactions on*, vol. 35, 1999.

[12] A. Pigazo, V. Moreno, and E. Estebanez, "A recursive park transformation to improve the performance of synchronous reference frame controllers in shunt active power filters," *IEEE Trans. Power Electron.*, vol. 24, no. 9, pp. 2065–2075, Aug. 2009.

[13] C.-S. Lam, W.-H. Choi, M.-C. Wong, and Y.-D. Han, "Adaptive dclink voltage-controlled hybrid active power filters for reactive power compensation," *IEEE Trans. Power Electron.*, vol. 27, no. 4, pp. 1758–1772, Apr. 2012.

[14] M. Monfared, M. Sanatkar, and S. Golestan, "Direct active and reactive power control of single-phase grid-tie converters," *IET Power Electron.*, vol. 5, no. 8, pp. 1544–1550, Nov. 2012.

[15] J. Hu, L. Shang, Y. He, and Z. Zhu, "Direct active and reactive power regulation of grid-connected DC/AC converters using sliding mode control approach," *IEEE Trans. Power Electron.*, vol. 26, no. 1, pp. 210–222, Jan. 2011.

[16] D. Zhi, L. Xu, and B. Williams, "Improved direct power control of grid-connected dc/ac converters," *IEEE Trans. Power Electron.*, vol. 24, no. 5, pp. 1280–1292, May 2009.

[17] M. Singh, P. Kumar, and I. Kar, "Implementation of vehicle to grid infrastructure using fuzzy logic controller," *IEEE Trans. Smart Grid*, vol. 3, no. 1, pp. 565–577, March 2012.

[18] K. Thirugnanam, T. Joy, M. Singh, and P. Kumar, "Modeling and control of contactless based smart charging station in v2g scenario," pp. 1–12, July 2013.

[19] M. Singh, P. Kumar, and I. Kar, "Designing a multi charging station for electric vehicles and its utilization for the grid support," *IEEE PES General Meeting (PESGM'12)*, pp. 1–8, July 2012.

[20] K. De Brabandere, B. Bolsens, J. Van den Keybus, A. Woyte, J. Driesen, and R. Belmans, "A voltage and frequency droop control method for parallel inverters," *IEEE Transactions on Power Electronics*, vol. 22, no. 4, pp. 1107–1115, Jul. 2007.

[21] K. Thirugnanam, H. Saini, and P. Kumar, "Mathematical modeling of li-ion battery for charge/discharge rate and capacity fading characteristics using genetic algorithm approach," *in Proc. IEEE Transportation Electrification Conf. and Expo (ITEC'12)*, pp. 1–6, June 2012.

[22] M. Aredes, H. Akagi, E. Watanabe, E. Vergara Salgado, and L. Encarnacao, "Comparisons between the p–q and p–q–r theories in three-phase four-wire systems," *IEEE Trans. Power Electron.*, vol. 24, no. 4, pp. 924–933, Apr. 2009.

[23] K. Deb, "Optimization for engineering design: Algorithms and examples," *Prentice Hall, India*, 1998.